

Marquette University
e-Publications@Marquette

Civil and Environmental Engineering Faculty
Research and Publications

Civil and Environmental Engineering, Department
of

11-1-2010

An Analytical Model of a Thermally Excited Microcantilever Vibrating Laterally in a Viscous Fluid

Stephen M. Heinrich

Marquette University, stephen.heinrich@marquette.edu

Rabin Maharjan

Marquette University

Isabelle Dufour

Université de Bordeaux

Fabien Josse

Marquette University, fabien.josse@marquette.edu

Luke A. Beardslee

Georgia Institute of Technology - Main Campus

See next page for additional authors

Accepted version. Published as part of the proceedings of the conference, *2010 IEEE Sensors*, 2011: 1399-1404. DOI. © 2010 Institute of Electrical and Electronics Engineers (IEEE). Used with permission.

Authors

Stephen M. Heinrich, Rabin Maharjan, Isabelle Dufour, Fabien Josse, Luke A. Beardslee, and Oliver Brand

An Analytical Model of a Thermally Excited Microcantilever Vibrating Laterally in A Viscous Fluid

Stephen Heinrich

*Department of Civil and Environmental Engineering
Marquette University
Milwaukee, WI*

Rabin Maharjan

*Department of Civil and Environmental Engineering
Marquette University
Milwaukee, WI*

Isabelle Dufour

*Université de Bordeaux, Laboratoire IMS
Talence, France*

Fabien Josse

*Department of Electrical and Computer Engineering
Marquette University
Milwaukee, WI*

Luke Beardslee

*School of Electrical and Computer Engineering, Georgia Tech
Atlanta, GA*

Oliver Brand

*School of Electrical and Computer Engineering, Georgia Tech
Atlanta, GA*

To achieve higher quality factors (Q) for microcantilevers used in liquid-phase sensing applications, recent studies have explored the use of the lateral (in-plane) flexural mode. In particular, we have recently shown that this mode may be excited electrothermally using integrated heating resistors near the micro-cantilever support, and that the resulting increase in Q helps to make low-*ppb* limits of detection a possibility in liquids. However, because the use of electrothermally excited, liquid-phase, microcantilever-based sensors in lateral flexure is relatively new, theoretical models are lacking. Therefore, we present here a new analytical model for predicting the vibratory response of these devices. The model is also used to successfully confirm the validity of our previously derived Q formula, which was based on a single-degree-of-freedom (SDOF) model and a harmonic tip force. Comparisons with experimental data show that the present model and, thus, the analytical formula provide excellent Q estimates for sufficiently thin beams vibrating laterally in water and reasonable upper-bound estimates for thicker beams.

Introduction

A. Background

Resonating microcantilever-based MEMS devices have been shown in recent years to provide a highly sensitive chemical sensing platform [1], [2]. Such devices operate on the principle that, if the microcantilever is coated with an appropriate chemically selective layer, its resonant frequency will decrease due to the sorption of analyte mass from the surrounding medium. Therefore, if one can successfully excite the cantilever into an observable resonant state and monitor any analyte-induced frequency shifts, the ambient concentration of the target substance may be correlated to the measured change in resonant frequency.

Conventional operation of resonant microcantilevers in sensing applications involves the excitation of transverse (out-of-plane) flexural vibrations, i.e., the beam vibrates out of the plane of the paper in Fig. 1a. This is typically the most flexible mode of vibration of

the microcantilever since the thickness h (out-of-plane dimension in Fig. 1a) is usually much less than the beam width (b). While the out-of-plane bending mode has been employed successfully for chemical sensing in air [3], [4], the use of this mode for detection in liquids is severely compromised primarily due to (a) large energy losses due to viscous dissipation in the liquid and, thus, low quality factors (Q) of the resonator and poor limits of detection, and (b) significantly lower resonant frequencies due to the large effective mass of the vibrating liquid and, thus, a large decrease in the analyte sensitivity of the device [5], [6].

Recent experimental work by our group [7] has indicated that the aforementioned obstacles associated with conventional (out-of-plane) use of microcantilevers in liquids may possibly be overcome by exciting the device in an in-plane, or "lateral," bending mode. (Such vibrations would occur in the plane of Fig. 1a, parallel to the beam width.) In that study the devices were excited electrothermally using integrated heating resistors near the beam support and the resulting vibration was monitored via a piezoresistive Wheatstone bridge. The device design is indicated in the SEM image and schematic of Fig. 1. The device response in water, as measured in [7], showed that the resulting increase in Q (relative to the transverse mode) could lead to low-*ppb* limits of detection in liquids. However, because the use of electrothermally excited, liquid-phase, microcantilever-based sensors in lateral flexure is relatively new, theoretical models are lacking. Therefore, we present here a new analytical model for predicting the vibratory response of these devices. The model is also used to successfully confirm the validity of our previously derived formula for the quality factor of thin microcantilevers vibrating in-plane, which was based on a simple single-degree-of-freedom (SDOF) model that assumed a harmonic tip force loading. As will be seen, comparisons with experimental data indicate that the present model and, thus, the analytical formula provide excellent Q estimates for sufficiently thin beams vibrating laterally in water and reasonable upper-bound estimates for thicker beams.

B. Motivation

In earlier theoretical work [8] we derived a simple model for lateral vibrations of a microcantilever in a viscous fluid when the excitation source is a harmonic tip force. That model assumed that the fluid resistance is due solely to shear stresses on the largest faces of the beam and that those stresses are given by Stokes's classical solution for an oscillating infinite plate [9], [10]. Our earlier model was relatively simple by virtue of a second assumption – namely, the beam was assumed to vibrate with a constant shape given by the first mode shape in vacuum. This resulted in a SDOF model whose solution yielded the following simple formula for the quality factor at resonance:

$$Q \approx 0.7124(E\rho_b^3/\eta^2\rho_f^2)^{1/4}(hb^{1/2}/L). \quad (1)$$

where h, b , and L are the thickness, width, and length of the cantilever, E and ρ_b are the effective Young's modulus and mass density of the beam material, and η and ρ_f are the viscosity and mass density of the surrounding fluid. However, formula (1) might not be applicable to the case of a device excited via electrothermal excitation near the support. We were therefore motivated to modify the previous model by (a) replacing the tip force with an "effective end rotation" near the support, which is a more realistic representation of the electrothermal excitation (see Figs. 1 and 2), and (b) making no assumptions *a priori* regarding the vibratory shape.

C. Specific Objectives

The specific objectives of the present paper are the following: (1) to derive a continuous-system model of an electrothermally excited microcantilever vibrating laterally in a viscous fluid; (2) to use the model to generate theoretical frequency response curves for arbitrary values of the system (beam/fluid) parameters; (3) to compare the resonant frequency predictions of the current model with those of our earlier SDOF model; (4) to compare the theoretical vibratory shape of the electrothermally excited beam with that assumed in the SDOF

model; and (5) to compare the quality factor predictions of the present model with those of the earlier model and with those measured in experiments of laterally vibrating microcantilevers in water.

Problem Statement

A. Idealized Problem

In order to represent the physical system (Fig. 1 a) with an idealized model that is amenable to analytical treatment, the following assumptions are made: (1) Bernoulli-Euler beam theory is valid, i.e., $b \ll L$; (2) the fluid is incompressible; (3) energies associated with modes other than lateral flexural are assumed to be negligible; (4) the electrothermal excitation induced by the heating resistors may be modeled as an equivalent end rotation prescribed at the support, which varies harmonically in time (Fig. 2); (5) the cross section is relatively thin, i.e., $h \ll b$, so that the fluid resistance associated with the pressure on the small faces (of dimension h) is negligible compared with that due to the shear resistance of the fluid on the large faces (of dimension b); and (6) the shear stress exerted by the fluid on the beam is uniform over the width dimension (b) and its magnitude is given by Stokes's classical unidirectional solution for harmonic, in-plane oscillations of an infinite plate in a viscous fluid [9], [10]. Assumption 4 has been confirmed via finite-element simulations and by appealing to the theory of bimetallic thermostats. We refer to the combination of assumptions 5 and 6 as the assumption of "Stokes fluid resistance," which should be valid for sufficiently thin beams.

The foregoing assumptions permit the problem of interest to be reduced to the analysis of the idealized system indicated in Fig. 3. The system parameters shown in Fig. 3 are defined as follows: $I = hb^3/12$ is the second moment of area of the beam cross section (corresponding to lateral bending); $\bar{m}_b = \rho_b bh$ is the beam's mass per unit length; θ_0 and ω are the amplitude and angular frequency of the effective end rotation due to the heating resistors; $\bar{m}_f(\omega)$ and $\bar{c}_f(\omega)$ are the frequency-dependent effective fluid mass per unit length and effective fluid damping coefficient per unit length (to be defined mathematically

in what follows); and $v(x,t)$ is the deflection of the beam corresponding to lateral bending. Our immediate goal is to relate the response of the system, $v(x,t)$, to the characteristics of the imposed end rotation and the system parameters.

B. Mathematical Formulation

The equation of motion for the bending deflection, $v(x,t)$, along the lateral direction (i.e., parallel to b) takes the form

$$EIV''(x,t) + [\bar{m}_b + \bar{m}_f(\omega)]\ddot{v}(x,t) + \bar{c}_f(\omega)\dot{v}(x,t) = 0, \quad (2)$$

which is accompanied by the boundary conditions (BCs)

$$v(0,t) = v'(L,t) = v''(L,t) = 0, v'(0,t) = \theta_0 e^{i\omega t}, \quad (3a-d)$$

where, employing the assumption of Stokes fluid resistance, the specific forms of the effective fluid properties are

$$\bar{m}_f = \frac{\sqrt{2\eta\rho_f b^2}}{\sqrt{\omega}} \quad (4a)$$

and

$$\bar{c}_f(\omega) = \sqrt{2\eta\rho_f b^2} \sqrt{\omega} \quad (4b)$$

For convenience, the boundary-value problem (BVP) is converted to the following dimensionless form:

$$\begin{aligned} \bar{v}''''(\xi, \tau) + \lambda^4 \left(1 + \frac{\zeta}{\lambda}\right) \ddot{\bar{v}}(\xi, \tau) + \lambda^3 \zeta \dot{\bar{v}}(\xi, \tau) &= 0 \\ \bar{v}(0, \tau) = \bar{v}'(1, \tau) = \bar{v}''(1, \tau) = 0, \bar{v}'(0, \tau) &= e^{i\tau} \end{aligned} \quad (6a-d)$$

where

$$\bar{v} \equiv \frac{v}{\theta_0 L}, \xi \equiv \frac{x}{L}, \tau \equiv \omega t \quad (7a-c)$$

$$\lambda \equiv \left(\frac{\bar{m}_b L^4 \omega^2}{EI}\right)^{1/4} \quad (7d)$$

$$\zeta \equiv \left(\frac{48\eta^2 \rho_f^2}{\rho_b^3 E}\right)^{1/4} \frac{L}{h\sqrt{b}} \quad (7e)$$

Note that λ is a normalized exciting frequency parameter and ζ is a normalized fluid resistance parameter.

Solution of BVP

As our main interest is the steady-state response of the system, a solution of (5) is sought in the form

$$\bar{v}(\xi, \tau) = X(\xi) e^{i\tau}, \quad (8)$$

where $X(\xi)$ will in general be complex. Then Eq. (5) becomes

$$X'''' - \kappa^4 X = 0 \quad (9)$$

with

$$\kappa = \kappa(\lambda, \zeta) \equiv \left[\lambda^4 \left(1 + \frac{\zeta}{\lambda}\right) - i\zeta\lambda^3\right]^{1/4}. \quad (10)$$

The general solution of (9) is

$$X(\xi) = A_1 \cosh \kappa \xi + A_2 \sinh \kappa \xi + A_3 \cos \kappa \xi + A_4 \sin \kappa \xi \quad (11)$$

Equation (8) implies that the BCs (6a-d) reduce to

$$X(0) = X''(1) = X'''(1) = 0, X'(0) = 1 \quad (12a-d)$$

Imposing these BCs on (11) gives the (complex) shape of the vibrating beam under an imposed (complex) harmonic end rotation $\theta_0 e^{i\omega t}$:

$$X(\xi) = \frac{1}{\kappa} \left[\sinh \kappa \xi + \frac{Cs - Sc}{2(1+Cc)} (\cosh \kappa \xi - \cos \kappa \xi) - \frac{1+Cc+Ss}{2(1+Cc)} (\sinh \kappa \xi - \sin \kappa \xi) \right], \quad (13)$$

where the following shorthand notation has been introduced:

$$C \equiv \cosh \kappa, S \equiv \sinh \kappa, c \equiv \cos \kappa, s \equiv \sin \kappa. \quad (14a-d)$$

The solution for the (complex) time-dependent deflection corresponding to (13) is given by (8).

In what follows we shall characterize the amplitude of vibration using the deflection at the free end of the beam. For this reason, we evaluate (13) at $\xi=1$ to obtain

$$X(1) = \frac{S+s}{\kappa(1+Cc)}. \quad (15)$$

It may be shown that the modulus of this complex amplitude may be interpreted as a "dynamic magnification factor" for the free-end ("tip") deflection, i.e.,

$$DMF_{tip} \equiv \frac{v_{max}(tip)}{L\theta_0} = |X(1)| = \left| \frac{S+s}{\kappa(1+Cc)} \right|, \quad (16)$$

where the denominator in the definition of DMF_{tip} is the maximum tip deflection corresponding to a slowly-applied (quasistatic) harmonic rotation at the left end. Plots of (16) as a function of dimensionless frequency λ (for fixed values of the fluid resistance parameter ζ) describe the frequency response of the tip deflection and will be presented in Section V.

Quality Factor

Having derived the beam response [(8) and (13)], the corresponding quality factor Q may be determined. The only energy losses that we shall consider in determining Q are those associated with viscous losses in the fluid. At an arbitrary driving frequency, the quality factor is defined in terms of energies as follows:

$$Q \equiv 2\pi \frac{(U+T)_{\max}}{\Delta W}, \quad (17)$$

with $(U+T)_{\max}$ being the maximum value of the beam's total energy (elastic U plus kinetic T) per cycle and ΔW is the energy lost to the surrounding fluid per cycle. If we consider the case of a real harmonic load of the form $\theta(\tau) = \theta_0 \cos \tau$, the corresponding response would be

$$\bar{v}(\xi, \tau) = \text{Re}[X(\xi) e^{i\tau}], \quad (18)$$

where $X(\xi)$ is given by (13). The corresponding beam energies may then be determined as follows:

$$U \equiv \frac{1}{2} EI \int_0^L [v''(x, t)]^2 dx = \frac{1}{2} \frac{EI\theta_0^2}{L} \int_0^1 [\bar{v}''(\xi, \tau)]^2 d\xi, \quad (19)$$

$$T \equiv \frac{1}{2} \bar{m}_b \int_0^L [\dot{v}(x, t)]^2 dx = \frac{1}{2} \bar{m}_b \omega^2 L^3 \theta_0^2 \int_0^1 [\dot{\bar{v}}(\xi, \tau)]^2 d\xi. \quad (20)$$

The energy lost to the fluid per cycle is equal to the work done in imposing the end rotation over one cycle (since the total beam energy does not change over one cycle of steady-state vibration):

$$\Delta W \equiv \int_0^{2\pi/\omega} [-EIv''(0, t)]d\theta = \frac{EI\theta_0^2}{L} \int_0^{2\pi} \bar{v}''(0, \tau) \sin\tau d\tau, \quad (21)$$

where the term in brackets represents the end couple needed to apply the prescribed end rotation. Substituting (18) into (19)–(21) yields

$$U = \frac{1}{2} \frac{EI\theta_0^2}{L} (\beta_1 \cos^2 \tau + \beta_2 \sin^2 \tau - 2\beta_3 \sin \tau \cos \tau), \quad (22)$$

$$T = \frac{1}{2} \bar{m}_b L^3 \omega^2 \theta_0^2 (\beta_4 \sin^2 \tau + \beta_5 \cos^2 \tau + 2\beta_6 \sin \tau \cos \tau), \quad (23)$$

$$\Delta W = \frac{\pi EI\theta_0^2}{L} \beta_7 \quad (24)$$

where the β_i are constants depending on λ and ζ . They are defined in terms of the complex shape $X(\xi)$ as follows:

$$\beta_1 \equiv \int_0^1 \{\text{Re}[X''(\xi)]\}^2 d\xi, \beta_2 \equiv \int_0^1 \{\text{Im}[X''(\xi)]\}^2 d\xi, \quad (25a, b)$$

$$\beta_3 \equiv \int_0^1 \text{Re}[X''(\xi)] \text{Im}[X''(\xi)] d\xi, \quad (25c)$$

$$\beta_4 \equiv \int_0^1 \{\text{Re}[X(\xi)]\}^2 d\xi, \beta_5 \equiv \int_0^1 \{\text{Im}[X(\xi)]\}^2 d\xi, \quad (25d, e)$$

$$\beta_6 \equiv \int_0^1 \text{Re}[X(\xi)] \text{Im}[X(\xi)] d\xi, \beta_7 \equiv -\text{Im}[X''(0)]. \quad (25f, g)$$

Placing (22)–(24) into (17) yields the quality factor Q :

$$Q(\lambda, \zeta) = \frac{\max[F(\tau, \lambda, \zeta)]}{\beta_7(\lambda, \zeta)} \quad (26)$$

where F is the normalized total beam energy, given by

$$F = F(\tau, \lambda, \zeta) = \beta_1 \cos^2 \tau + \beta_2 \sin^2 \tau - 2\beta_3 \sin \tau \cos \tau + \lambda^4 (\beta_4 \sin 2\tau + \beta_5 \cos^2 \tau + 2\beta_6 \sin \tau \cos \tau). \quad (27)$$

A computer program has been written to evaluate (26), the results of which will be presented in the following section. Note that (26) is valid for an *arbitrary* value of frequency parameter λ ; however, of particular interest is the value of Q at resonance, i.e., at a value of λ corresponding to a resonant peak. In the following section, results for Q corresponding to the first resonant peak in lateral flexure will be given.

Numerical Results and Discussion

Frequency Response

Equation (16) has been plotted in Fig. 4 to illustrate the frequency response of the system for arbitrary values of the frequency (λ) and fluid (ζ) parameters. Note that the continuous model of the system is capable of capturing all resonant peaks in lateral flexure, unlike our earlier SDOF model. The results of Fig. 4 indicate that both the resonant peak magnitude and its sharpness (Q) are reduced at the higher resonances, thus suggesting that the first resonant mode may be the most promising of the lateral flexural modes for sensing applications using the type of device considered.

Resonant Frequency

From the plots of Fig. 4 it is clear that, according to the model, the resonant values of the frequency parameter depend only on the fluid resistance parameter. This relationship is plotted in Fig. 5 for the first resonant peak. Although values of ζ up to 10 are considered in the figure for generality, most beams at the micro-scale in liquids similar to water will correspond to values of ζ in the range $[0, 0.2]$. For such systems, Fig. 5 indicates that the Stokes resistance of the liquid will reduce the resonant frequency by no more than a few percent when

2010 IEEE Sensors Proceedings, (November 1-4, 2010): pg. 1399-1404. [DOI](#). This article is © Institute of Electrical and Electronics Engineers (IEEE) and permission has been granted for this version to appear in e-Publications@Marquette. Institute of Electrical and Electronics Engineers (IEEE) does not grant permission for this article to be further copied/distributed or hosted elsewhere without the express permission from Institute of Electrical and Electronics Engineers (IEEE).

the beam resonates in lateral flexure. Also indicated in the figure are the results of our earlier SDOF model. While the resonant frequency results of the two models are very similar, one should note that these models are based on the assumption of Stokes fluid resistance and will therefore underestimate the frequency drop due to the fluid. To obtain better frequency estimates in fluids (especially in liquids), the pressure resistance on the smaller faces of the beam should be taken into account. However, even when pressure effects are considered, the fluid-induced drop will be much less than that associated with transverse flexural vibrations in liquids.

Quality Factor (at first resonant peak)

Evaluating (26) at the first resonant frequency for various values of ζ leads to the Q results (solid curve) plotted in Fig. 6. For comparison purposes the approximate analytical formula for Q based on our earlier SDOF model is also plotted. Over the range of ζ considered, the analytical formula (1) based on the simple model does an excellent job of approximating the more exact results of the continuous model. Also of note is that Fig. 6 may be useful from a design standpoint: given a desired Q value, one may determine how small the value of ζ must be to achieve it. If the fluid properties are known, (7e) may then be used to determine the necessary beam dimensions and/or material properties.

Vibratory Shape (at first resonant peak)

We have seen that, for the determination of the resonant frequency and quality factor at the first lateral resonance, the SDOF model (based on an applied force loading) gives results that are in excellent agreement with those of the continuous model (based on an imposed support rotation loading). Therefore, it is reasonable to suppose that the more exact vibratory shape as calculated in the present model is quite similar to the shape assumed in the SDOF model (i.e., the first mode of a cantilever in vacuum). To confirm this conjecture, the envelope of the time-dependent beam shapes at first resonance for $\zeta=0.2$, as predicted by the current model, has been plotted in Fig. 7, along with the constant shape assumed in the SDOF

2010 IEEE Sensors Proceedings, (November 1-4, 2010): pg. 1399-1404. [DOI](#). This article is © Institute of Electrical and Electronics Engineers (IEEE) and permission has been granted for this version to appear in e-Publications@Marquette. Institute of Electrical and Electronics Engineers (IEEE) does not grant permission for this article to be further copied/distributed or hosted elsewhere without the express permission from Institute of Electrical and Electronics Engineers (IEEE).

model. (The rigid rotation portion of the beam deflection was removed when determining the shape envelope in Fig. 7, so that only the portion associated with bending was considered.) Clearly, the shapes are very similar, explaining why the SDOF model gives similar results for the first-peak resonant characteristics in the range $\zeta \in [0, 0.2]$. However, preliminary investigations indicate that the agreement may deteriorate at higher modes or at larger ζ values.

Quality Factor: Theory vs. Experiment

The values of Q calculated by the present model and the analytical formula are compared with preliminary data in Fig. 8. Details concerning the experiments, performed on Si beams in water, may be found in [5]. Values used in the models are the following:

$\rho_b = 2330 \text{ kg/m}^3, \rho_f = 1000 \text{ kg/m}^3, \eta = 0.00089 \text{ Pa}\cdot\text{s}$. Two sets of data were generated corresponding to specimens having nominal Si thicknesses of 8 μm and 12 μm . After the addition of passivation layers, the average total thickness values of 10.33 μm and 14.48 μm , respectively, were used as h values. For these two data sets, the respective values of effective modulus E were 90.8 and 87.0 GPa. (These values were based on fitting resonant frequency data in air.)

Figure 8a shows the Q comparison for the thinner set of beams. Agreement between theory and experiment is quite good, indicating that the specimen dimensions in this set are such that Stokes fluid resistance may indeed be the dominant contributor to energy dissipation. In Fig. 8b, however, we see that the agreement is not as good for the thicker beam set, most likely due to the pressure effects on the smaller beam faces which have been ignored in the models. Nevertheless, the theoretical results provide a reasonable upper-bound estimate of Q for most of the thicker specimens. Qualitatively, the experimental trends of Figs. 8a, b support the theoretical results — namely, that Q should increase as b and h are increased and as L is decreased.

Summary and Conclusions

A new model has been derived for an electrothermally driven microcantilever experiencing in-plane flexural vibrations in a fluid. The beam has been modeled as a continuous system, making the present model a generalization of the authors' earlier SDOF model. The present model treats the electrothermal loading in a more realistic manner (as an effective support rotation) compared with the tip-force loading of the earlier model. The new model has certain advantages over the SDOF model, including the ability to determine (a) beam response for arbitrary values of driving frequency, beam dimensions/properties, and fluid properties; (b) resonant frequency and quality factor at several resonant peaks in lateral flexure (not only at the first peak); and (c) the time-dependent shape of the vibrating beam. Despite these improvements over the SDOF model, the new model has validated the accuracy of the SDOF results when applied to the first resonant state in lateral flexure over the range of fluid resistance parameter (ζ) considered. In particular, very good agreement was found between the fundamental resonant frequency and quality factor predictions of the SDOF model and the more exact continuous model at values of ζ representative of microscale beams excited laterally in water. When compared with experimental data in water, both models predicted the quality factor extremely well for relatively thin beams (i.e., for those cases in which the Stokes fluid resistance assumption is expected to be valid), while giving reasonable upper-bound estimates for Q as the beam thickness was increased.

References

1. M. Sepaniak, P. Datskos, N. Lavrik, C. Tipple, "Microcantilever transducers: a new approach in sensor technology", *Analytical Chemistry*, vol. 74, pp.568-575, 2002
2. K. Goeders, J. Colton, L. Bottomley, "Microcantilevers: sensing chemical interactions via mechanical motion", *Chemical Reviews*, vol. 108, pp.522-542, 2008

- 3.** P. S. Waggoner, H. G. Craighead, "Micro- and nanomechanical sensors for environmental chemical and biological detection", *Lab on a Chip*, vol. 7, pp.1238-1255, 2007
- 4.** D. Lange, C. Hagleitner, A. Hierlemann, O. Brand, H. Baltes, "Complementary metal oxide semiconductor cantilever arrays on a single chip: mass-sensitive detection of volatile organic compounds", *Analytical Chemistry*, vol. 74, pp.3084-3095, 2002
- 5.** L. Beardslee, "Thermal excitation and piezoresistive detection of cantilever in-plane resonance modes for sensing applications", *Journal of Microelectromechanical Systems*, pp.3, 2010
- 6.** C. Vancura, J. Lichtenberg, A. Hierlemann, F. Josse, "Characterization of magnetically actuated resonant cantilevers in viscous fluids", *Appl. Phys. Lett.*, vol. 87, no.162510, 2005
- 7.** L.A. Beardslee, "Liquid-phase chemical sensing using lateral mode resonant cantilevers", *Analytical Chemistry*, 2010
- 8.** S.M. Heinrich, "An analytical model for in-plane flexural vibrations of thin cantilever-based sensors in viscous fluids: applications to chemical sensing in liquids", pp.2
- 9.** G.G. Stokes, "On the effect of the internal friction of fluids on the motion of pendulums", *Trans. Camb. Phil. Soc.*, vol. 9, pp.8-106, 1851
- 10.** F. White, McGraw-Hill, 2006

Figures

Figure 1. Electrothermally excited microcantilever: (a) SEM image; (b) schematic of heating resistors and piezoresistive Wheatstone bridge for vibration detection.

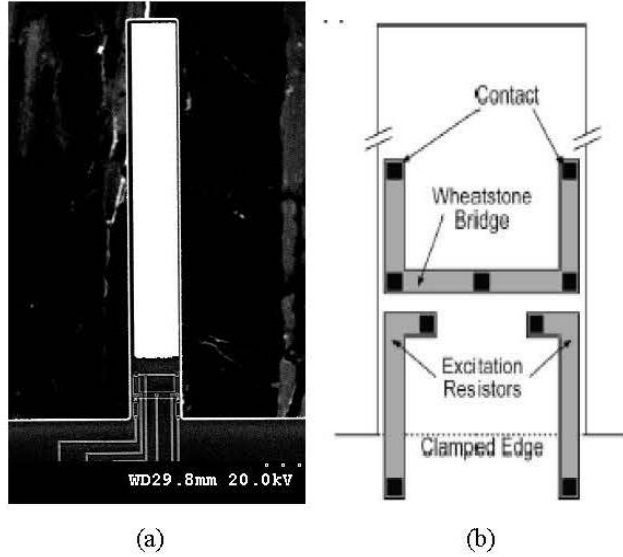


Figure 2. Idealized model for lateral excitation of microcantilever: (a) thermal load of heating resistors; (b) equivalent end rotation. E =Young's modulus, ω =exciting frequency, η =fluid viscosity, and ρ_b, ρ_f = mass densities.

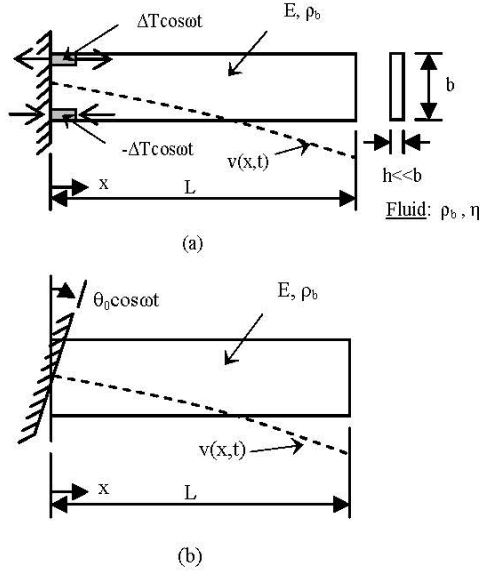


Figure 3. Idealized model for electrothermal excitation, including effect of fluid resistance as distributed fluid mass and distributed fluid damping.

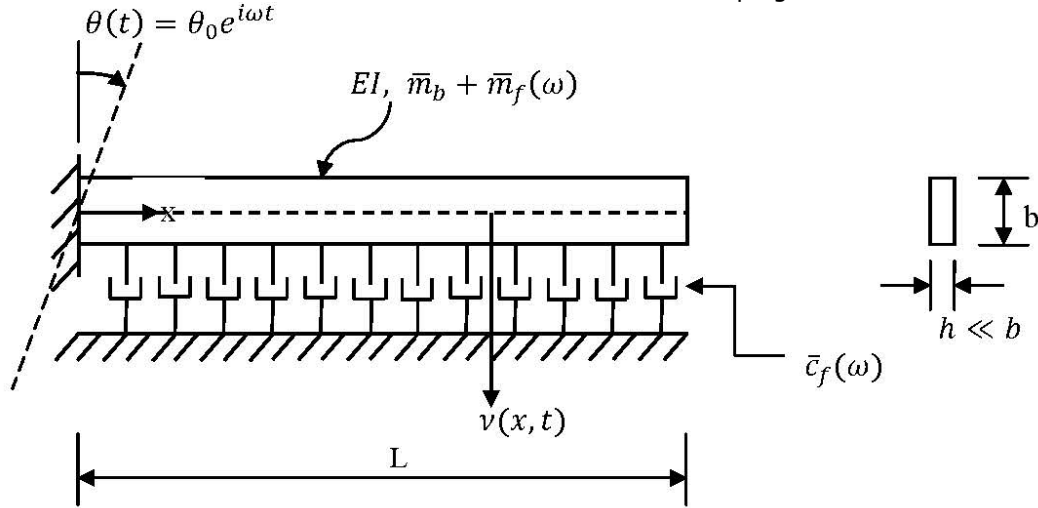


Figure 4. Theoretical frequency response of cantilever tip for lateral vibration of microcantilever in fluid caused by electrothermal excitation at the support. Parameters λ and ζ are the dimensionless frequency and fluid resistance parameters defined in Eqs. (7d, e).

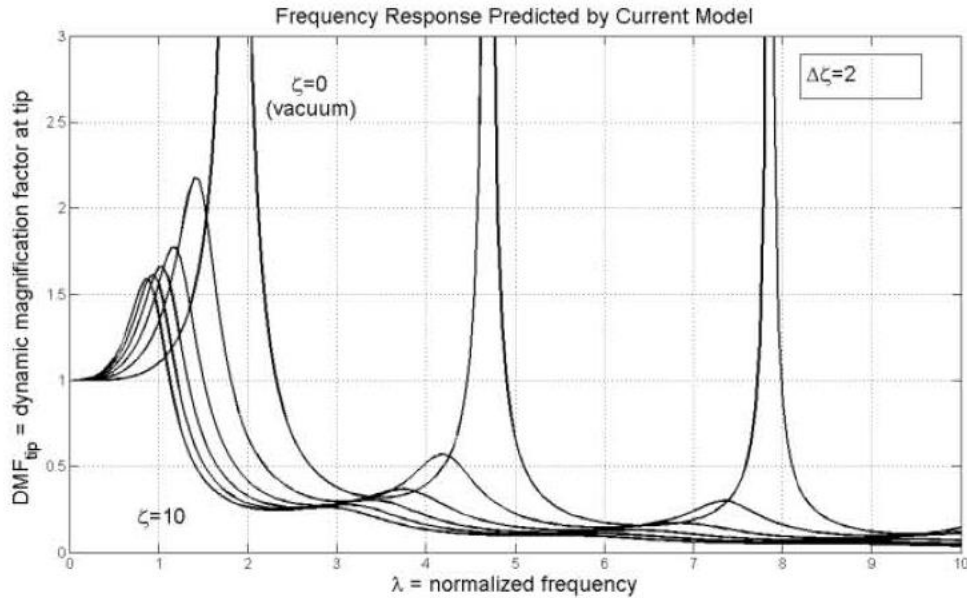


Figure 5. Comparison of resonant frequency predictions of current model and previous SDOF model.

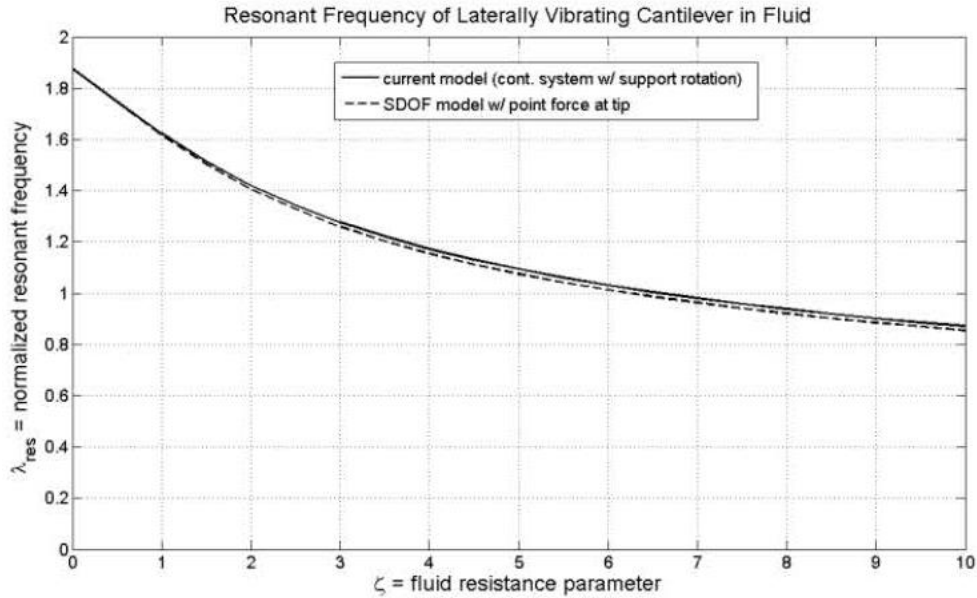


Figure 6. Comparison of quality factor predictions (at first lateral resonance) of current model and approximate analytical formula based on SDOF model with tip force loading.

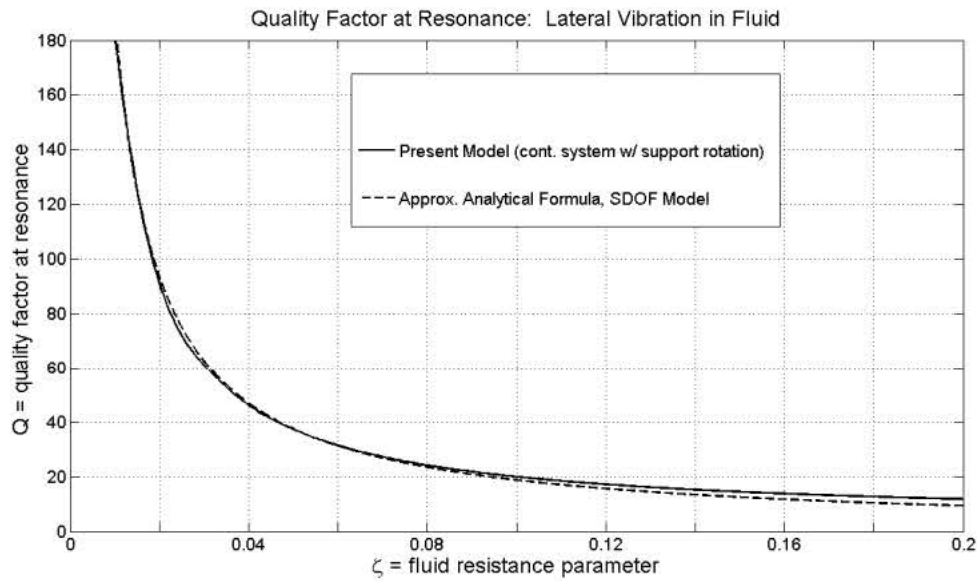


Figure 7. Deformed Beam Shape at First Resonant Peak for $\zeta=0.2$: The beam shape in fluid, as predicted by the present model, depends on time and lies within the two solid curves shown. Discrete markers denote the (time-independent) first mode shape for a cantilever in vacuum.

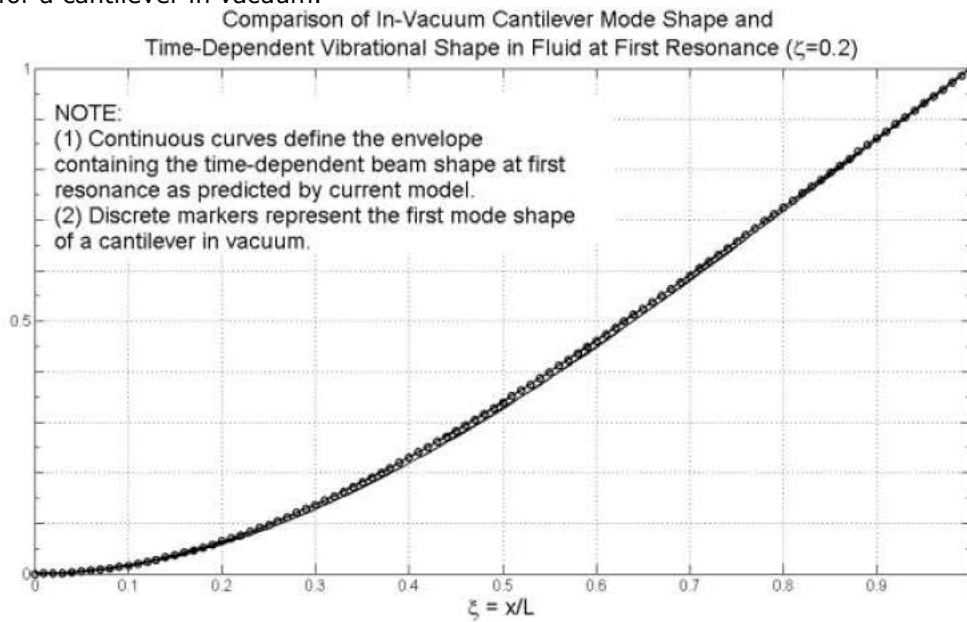
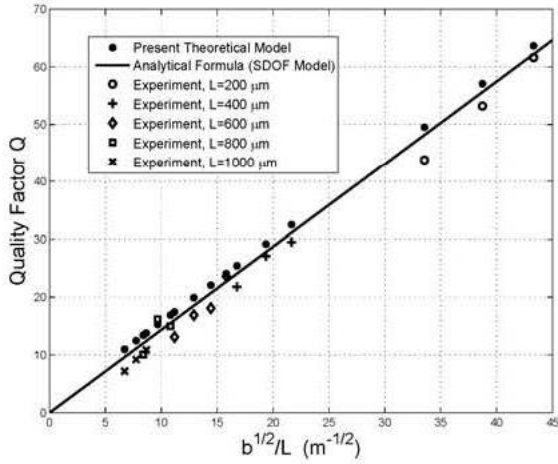
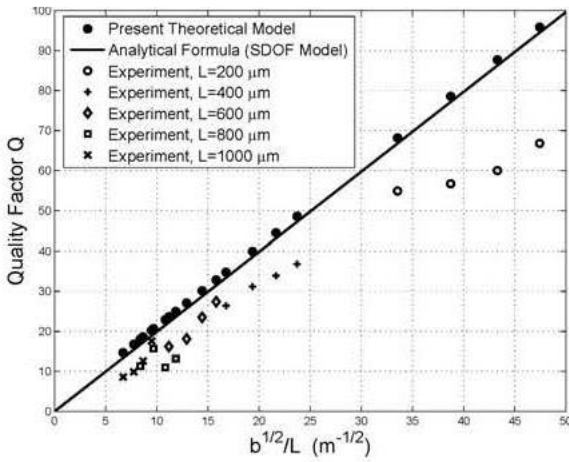


Figure 8. Quality factor comparisons: current model, SDOF model (analytical formula), and experimental data (in water): (a) nominal Si thickness = 8 μm ; (b) nominal Si thickness = 12 μm .



(a)



(b)